ELSEVIER

Solid State Ionics 69 (1994) 212–221

SOLID STATE IONICS

Lithium-ion rechargeable batteries with $LiCoO_2$ and carbon electrodes: the $LiCoO_2$/C system

Kazunori Ozawa

Sony Corporation, Battery Group, 6-7-35 Kitashinagawa, Shinagawa-ku, Tokyo, Japan

Abstract

Lithium-ion rechargeable battery with $LiCoO_2$ cathode and non-graphitizable carbon anode has high energy density (253 Wh/ℓ in 18650). By using $LiPF_6$ containing propylene carbonate/diethyl carbonate electrolyte solution, excellent cycle performance can be obtained even at a moderately high temperature, because (1) $LiCoO_2$ remains stable, and (2) non-graphitizable carbon exhibits a good cyclability with respect to Li-doping/undoping capability. Although a thin film is formed on the carbon surface during charge and discharge cycling, the discharge capacity degradation is only 10 to 20% after 500 cycles. Furthermore, even if the cell is overcharged, safety can be attained (1) by providing an anti-overcharging safety device which operates when Li_2CO_3 in the cathode is decomposed and (2) by using a polyolefin separator which shuts down at a high temperature due to overcharge current.

1. Introduction

Lithium ion rechargeable batteries with lithium carbon intercalation compounds (Li-CIC) have achieved high energy density, excellent cycle life and sufficient safety characteristics. These lithium ion rechargeable batteries of $LiCoO_2$/C system [1,2], whose sizes are 14500 (14 mm in diameter and 50 mm in height) and 20500 (20 mm in diameter and 50 mm in height), were first introduced for the portable telephone (HP-211) in June 1991 by Sony Corporation. Recently, 18650 (18 mm in diameter and 65 mm in height), was introduced for 8 mm video tape recorders. Furthermore, we have developed a newly improved lithium ion rechargeable battery using non-graphitizable carbon, $LiCoO_2$ containing a little amount of Li_2CO_3 (the function of Li_2CO_3 is explained in Section 3) and PC+DEC/$LiPF_6$ electrolyte solution. In this paper the key materials for this cell and the cell construction are explained. Some properties of this cell such as charge characteristics, discharge drain capability, temperature dependence of discharge capacity, cycle life, and safety characteristics are also described. In addition, the state of the doped lithium in the carbon and the surface of carbon material during charge–discharge was investigated in order to clarify the deterioration of the lithium ion rechargeable battery. In conclusion, the characteristics of lithium ion rechargeable batteries, which are available on the market, are summarized.

2. Chemistry and materials

2.1. Lithium-containing transition metal oxides for a cathode

For layered transition metal oxides $LiMO_2$ (M=Co, Ni) and spinel manganese oxide $LiMn_2O_4$, electrode potentials become higher than 4 V versus Li/Li^+ by extracting lithium from these oxides electrochemically in a nonaqueous electrolyte solutions

0167-2738/94/$07.00 © 1994 Elsevier Science B.V. All rights reserved
SSDI 0167-2738(94)00042-Q

RJ Technology Exhibit 2014
Apple Inc. v. RJ Technology LLC
IPR2023-01350, Page 1 of 10

[3–7]. Fig. 1 shows the low rate charge and discharge curves of coin type cells with an excess amount of metallic lithium and propylene carbonate (PC) + 1,2-dimethoxyethylene (DME)/$LiPF_6$ electrolyte solution. As shown in this figure, it is found that lithium intercalation/deintercalation into/from these oxides take place at the potential around 4 V. Particularly, in the case of $LiCoO_2$, the polarization is smaller and the capacity is larger compared with other transition metal oxides [8,9]. Accordingly, it is necessary to employ a transition metal oxide with high capacity and high electrode potential, such as $LiCoO_2$, as a cathode in order to attain the higher energy density.

However, cycle performance strongly depends on the electrolyte solution. Fig. 2 shows the cycle performance of the $LiCoO_2$ cathode by using the coin type cell with an excess amount of metallic lithium. As shown in this figure, it was found that the retention of the discharge capacity in the case of PC + DME/$LiPF_6$ decreases notably with increasing cycle number. On the other hand, it was found that by using PC + dimethyl carbonate (DMC)/$LiPF_6$, the degradation of discharge capacity can be suppressed. As the electrochemical stability of PC + DMC/$LiPF_6$ is higher than that of PC + DME/$LiPF_6$, it is considered that the improvement of the cycle performance could be attained by using an electrolyte system with high electrochemical stability.

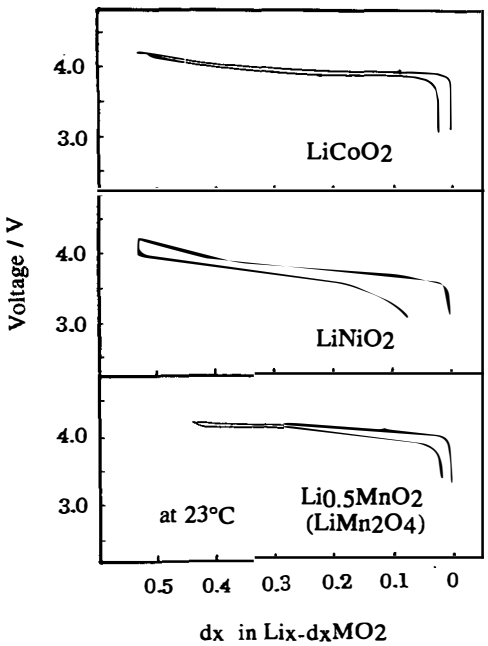

Fig. 1. Charge and discharge curves of Li/$Li_{x-dx}MO_2$ (M = Co, Ni and Mn). Charge: maximum limit of 4.2 V; discharge: 3.3 V cut-off; current density: 0.5 mA/cm².

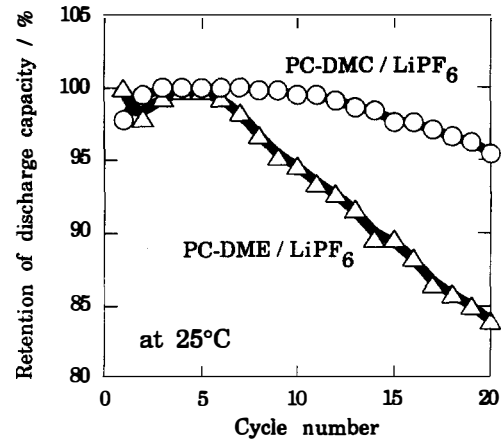

Fig. 2. Cycle performances of Li_xCoO_2 in PC-DME nd PC-DMC/$LiPF_6$ electrolytes. Charge: maximum limit of charge to 4.2 V; discharge: 3.7 V cut-off; current density: 0.5 mA/cm².

2.2. Carbon materials for an anode

By using carbon materials as an anode for lithium ion rechargeable batteries, carbon can be lithium-doped/undoped during charging/discharging without a morphology change at the surface. The reaction of Li-CIC during charge–discharge can be expressed as the following equation:

$$Li_xC \underset{\text{charge}}{\overset{\text{discharge}}{\rightleftharpoons}} Li_{x-dx}C + dx\cdot Li^+ + dx\cdot e^- .$$

Since this reaction is reversible and the $LiCoO_2$ cathode is also a lithium intercalation compound which can be lithium doped/undoped without a morphology change, the long cycle life can be attained.

Graphite is distinguished from carbon materials because of its high crystallinity. It is well known to react with lithium to form lithium graphite intercalation compounds (Li-GIC). Carbon materials are classified into two categories according to the structure characteristics: graphitizable carbon and non-graphitizable carbon. Franklin [10] illustrated a model of each structure as shown in Fig. 3. Compared with graphitizable carbon, non-graphitizable carbon generally has low density, porous surface, small crystallites, relatively random orientation of

RJ Technology Exhibit 2014
Apple Inc. v. RJ Technology LLC
IPR2023-01350, Page 2 of 10

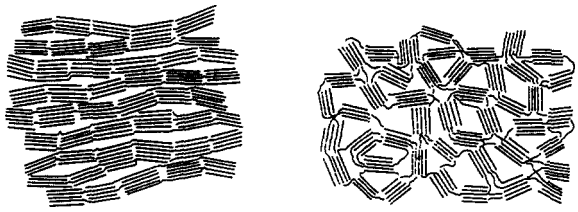

(a) graphitizable carbon (b) non-graphitizable carbon

Fig. 3. Structure models of carbon materials proposed by Franklin [10].

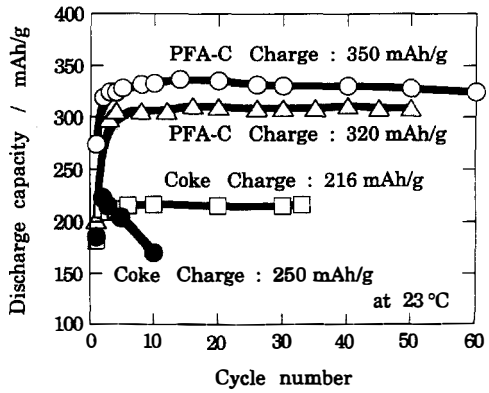

Fig. 4. Cycle performances of heat-treated polyfurfuryl alcohol (PFA-C) and acenaphthylene derived pitch coke. Cathode: $Li_xNi_yCo_{1-y}O_2$; electrolyte: PC-DME 1M $LiClO_4$; current density: 0.5 mA/cm^2.

crystallites and long interplanar spacing (d_{002}). Since graphitizable carbon is similar to graphite with respect to crystallinity, lithium intercalation into the graphitizable carbon seems to be preferable to that of non-graphitizable carbon.

Coke, which is a typical graphitizable carbon, had been widely investigated in the early stage of research in anode materials [11]. It has been revealed that Li-GIC can be electrochemically synthesized in ethylene carbonate (EC) based non-aqueous electrolyte solution. Therefore, graphite can be used as an anode for lithium secondary batteries. The capacity of coke is inferior to that calculated from the formula of first stage Li-GIC (C_6Li), 372 mAh/g. Accordingly, it was strongly desired to improve lithium doping/undoping capabilities of carbon materials in order to attain the higher energy density.

Polyfurfuryl alcohol derived carbon (PFA-C) is a typical material of non-graphitizable carbon. Fig. 4 shows the comparison of cycle performances of coke and PFA-C, which were obtained by charge and discharge cycling with a constant current by charging up to a constant capacity. Coke retains its discharge capacity when charged up to 216 mAh/g, though the degradation is observed when charged up to a larger capacity (250 mAh/g). On the other hand, PFA-C shows good cycling behavior even when charged up to 350 mAh/g, which is close to the capacity corresponding to C_6Li (372 mAh/g). Accordingly, it was clarified that non-graphitizable carbon such as PFA-C is a very useful anode material for lithium-ion rechargeable batteries [12–16].

Lithium doping/undoping capabilities depend strongly on the species of carbon materials. Even though the same carbon precursor is selected, the carbon obtained by heat-treatment with various temperatures yield numerous kinds of structures, depending on the carbonization processes. Furthermore, the capacity is considered to be affected by the characteristics of structures such as stacking structure and/or alignment of crystallites. Since the structure of non-graphitizable carbon (glassy-like carbon) can be modified in various ways, there are still many possibilities to increase the capacity by optimizing the structure related to lithium doping/undoping capabilities.

2.3. Nonaqueous electrolyte solution

A study on the behavior of lithium metal at the overcharging potential range revealed that the electrolyte system using $LiPF_6$ as a lithium salt shows good performances. "Dendritic" lithium does not deposit in this system, but "spherical" lithium deposits as shown in Fig. 5. [17]. In the PC/$LiPF_6$ system, absorbates derived from $LiPF_6$ are formed on the electrode surface, which prevent the reaction of the electrolyte with metallic lithium. These absorbates might affect the morphology of the deposited lithium. As shown in Fig. 5, diameter of deposited "spherical" lithium was about 1 μm. However, with decrease in $LiPF_6$ concentration, the shape of deposited lithium changed from "spherical" to "columnar". Therefore the $LiPF_6$ concentration of 1 M was selected in PC solvent.

In these rechargeable batteries with high voltage, it is also required that the electrolyte solution remain stable at a voltage higher than 4 V, in the temperature

RJ Technology Exhibit 2014
Apple Inc. v. RJ Technology LLC
IPR2023-01350, Page 3 of 10

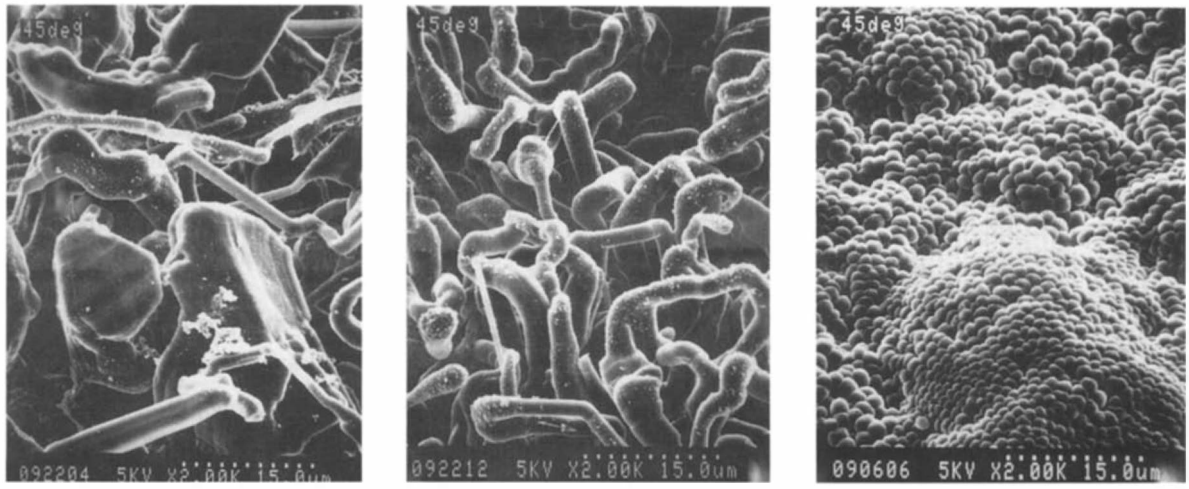

Fig. 5. Dependence of the Li morphology on Li salts in the electrolyte system (a) $LiClO_4$; (b) $LiAsF_6$; (c) $LiPF_6$. Solvent: PC/DME, current density: 0.33 mA/cm^2, substrate: Cu.

range of approximately −20 to +60°C. As a result of investigating various nonaqueous electrolyte solutions, it was found that these requirements could be met by using PC+diethyl carbonate (DEC)/$LiPF_6$.

Fig. 6 shows cycle performances of cylindrical cells with wound electrodes. The lithium ion rechargeable battery using PC-DME/$LiPF_6$ exhibits the excellent cycle performance around 23°C comparatively. However, with increasing temperature, the cycle performance becomes worse as shown in Fig. 6. On the other hand, PC-DEC/$LiPF_6$ exhibits a smaller decrease in the retention of the discharge capacity even at a moderate high temperature (45°C) [18]. It is considered that the cycle performance could be improved using the electrolyte solution with electrochemical stability such as PC+DEC/$LiPF_6$. Furthermore, the boiling point of PC+DEC/$LiPF_6$ is higher than that of PC+DMC/$LiPF_6$. Thus, in order to operate at various temperatures, it is desirable that PC+DEC/$LiPF_6$ be employed for the lithium ion rechargeable battery.

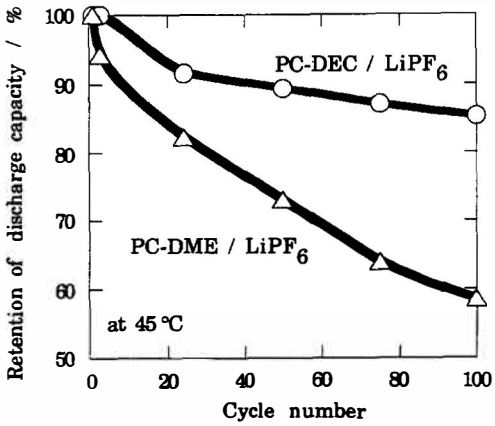

Fig. 6. Effect of electrolyte on cycle performance. Charge: maximum limit of 4.1 V, 1 A, 2.5 h; discharge: 2.7 V cut-off.

3. Cell construction

The conductivity of nonaqueous electrolytes used for the lithium ion rechargeable battery is lower than that of aqueous electrolyte used for Ni–Cd batteries by two orders of magnitude. To make up for the low conductivity of nonaqueous electrolytes, larger surface area electrodes and thinner, mechanically stronger separator are necessary. A multiple wound structure with thin electrodes is a technical way to increase surface areas of the electrodes. Fig. 7 illustrates a construction of the lithium ion rechargeable battery. Polyolefin separator, whose thickness is around 25 μm and melting point is around 140°C, can contribute for the safety of the battery, since it

RJ Technology Exhibit 2014
Apple Inc. v. RJ Technology LLC
IPR2023-01350, Page 4 of 10

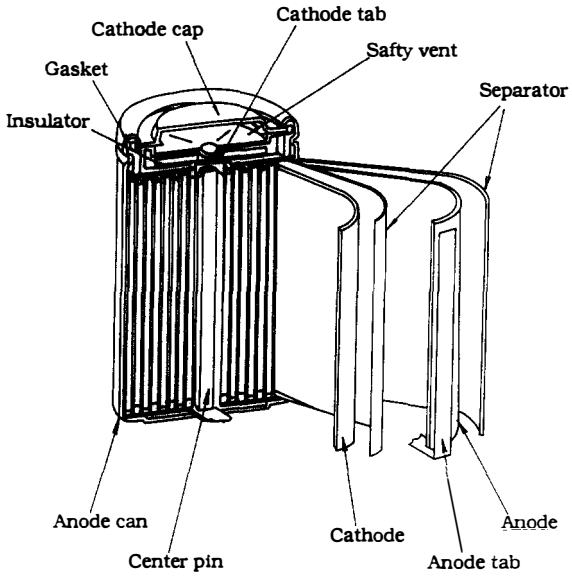

Fig. 7. Cell construction.

melts down and shuts off the rush current when the cell temperature rises with abuse such as short circuiting. The cells are prevented from reaching high internal temperature, namely the melting point of lithium (180.5°C).

Lithium ion rechargeable batteries made by Sony Corporation contain anti-overcharging safety device as shown in Fig. 8. This device is activated with the increase of internal pressure of the cell when the control of the charging is lost. When the cell voltage exceeds 4.7 V, internal pressure gradually increases due to the decomposition of excess amounts of Li_2CO_3. The internal pressure quickly increases at above approximately 5.0 V. In accordance with these phenomena, the aluminum burst disk bulges and the aluminum lead disconnects from the cell element. The presence of excess Li_2CO_3 does not affect the current flow during normal operation of the cell.

4. Characteristics

4.1. Charge–discharge performance

Fig. 9 shows a typical charging profile of the lithium ion rechargeable battery. The following data were mainly taken with 20500 size cell. As the charge capacity of this battery depends on the quantity of lithium ions extracted from the cathode, the lithium ion rechargeable battery must be charged to a maximum voltage (usually 4.2 V) with a constant current. When charging with 1.0 A, cell voltage gradually increases and reaches the maximum limited voltage within about 30 min, while the charging current begins to decrease and reaches about tens of mA within two hours. It takes about an hour to charge 80% of the maximum capacity. Fig. 10 shows the charge current dependence of charge capacity. In the case of 2.0A charge, more than 90% of the maximum capacity is charged within an hour. Thus, the lithium ion rechargeable battery can be quickly and simply charged

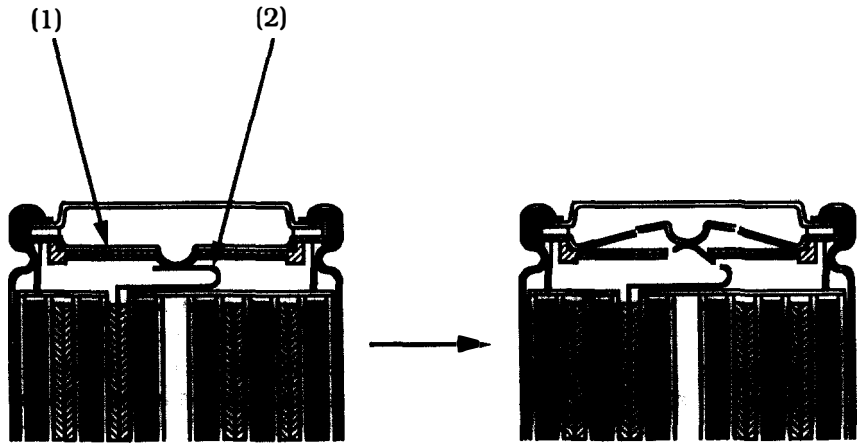

Fig. 8. Current breaker mechanism as well as a vent mechanism for an abnormal rise of internal pressure in case of over-charging with no voltage limiting: (1) aluminum burst disk; (2) aluminum lead.

RJ Technology Exhibit 2014
Apple Inc. v. RJ Technology LLC
IPR2023-01350, Page 5 of 10

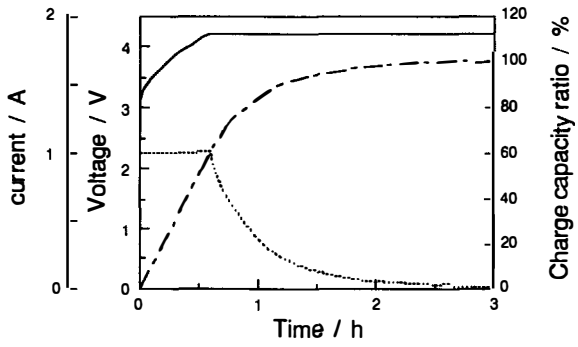

Fig. 9. Typical charge profiles of a lithium ion rechargeable battery. Charge: max. limit 4.2 V, 1 A. (——) voltage; (– – –) charge capacity; (—) current. Diameter; 20 mm; height: 50 mm. Electrolyte solution: PC-DEC/Li PF_6.

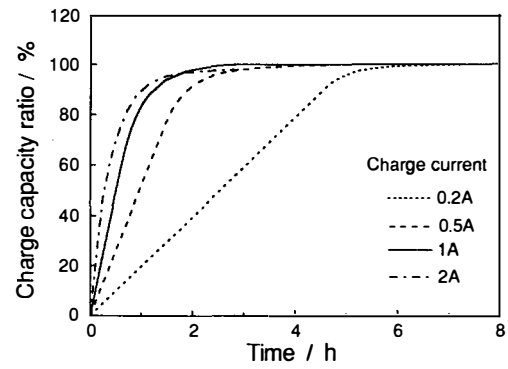

Fig. 10. Charge characteristics of a lithium ion rechargeable battery. Charge: max. limit 4.2 V.

to the limited maximum charging voltage.

Fig. 11 shows the temperature dependence of charge capacity with 200 mA charge. There is little difference in the charge capacity for the cells charged at temperatures from 0°C to 40°C.

Fig. 12 shows the typical discharge curves obtained by a constant current discharge of 200 mA (0.2C rate). The discharge capacity and energy density are 1000 mAh and 220 Wh/l, respectively. The lithium ion rechargeable battery with this capacity shows a high average voltage of about 3.6 V, which is three times as high as that of the Ni–Cd battery. When an application requires an operating voltage ranging from 3 to 4 V, three Ni–Cd batteries are required to be connected in series. However, only one lithium ion rechargeable battery is needed for the same application. Moreover, it is possible to monitor the remaining discharge capacity because the cell voltage decreases gradually during discharge.

Fig. 13 shows the drain capability of the lithium ion rechargeable battery. Before each discharge, cells are charged with 1.0 A for 2.5 h up to the maximum limit of 4.2 V. Output capacities at 700 mA and 1400 mA discharges are 96% and 89% of the capacity at 200 mA discharge, respectively. In particular, discharge capacity below 1000 mA has little dependence of the discharge current and is more than 90% of the nominal capacity. Furthermore, even at 3000 mA discharge current, 60% of the nominal capacity is obtained.

Particular interest for rechargeable batteries is the ability of the battery when discharged at low temper-

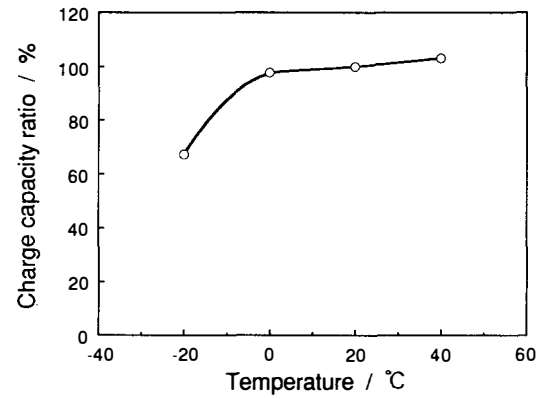

Fig. 11. A temperature dependence of charge capacity. Charge: max. limit 4.2 V, 1 A, 5 h (charge capacity at 20°C = 100%).

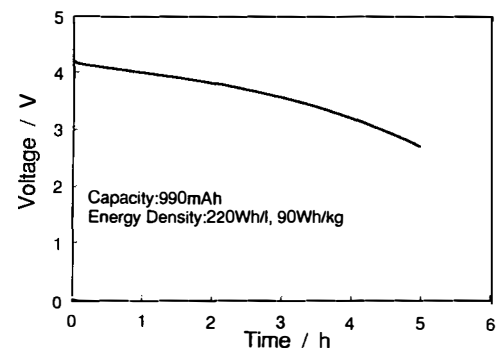

Fig. 12. A typical discharge curve of a lithium ion rechargeable battery. Discharge: 2.75 V cut off, 0.2 A.

RJ Technology Exhibit 2014
Apple Inc. v. RJ Technology LLC
IPR2023-01350, Page 6 of 10

atures. Temperature dependence of discharge capacity is shown in Fig. 14. Cells were charged with a charging current of 1.0 A for 2.5 h up to 4.2 V at 20°C ambient temperature, then discharged at various temperatures at a constant current of 200 mA to a cutoff voltage of 2.75 V. Even at −20°C, 83% of the discharge capacity at 20°C was available. As the low temperature capability is almost the same with conventional Ni–Cd batteries, there is no problem to apply this battery practically.

Fig. 15 shows the change in retention of the energy density plotted against cycle number. Although the decrease of capacity with increasing cycle number is observed depending on the discharge rate, the retention of energy density is 90% of the initial energy density after 500 cycles at 0.35C discharge rate and 80% at 1.0C. These data were obtained at 100% DOD (depth of discharge). By cycling with smaller DOD, the cycle life of the battery can be further extended. The cycle life also depends on the ambient temperature. Although the cycle life becomes shorter, in general has little dependence on the discharge current, the lithium ion rechargeable battery using PC+DEC/$LiPF_6$ electrolyte system shows an excellent cycle performance as shown in Fig. 15. About 90% of the initial energy density remains after 500 cycle, and also about 85% remains even at 45°C.

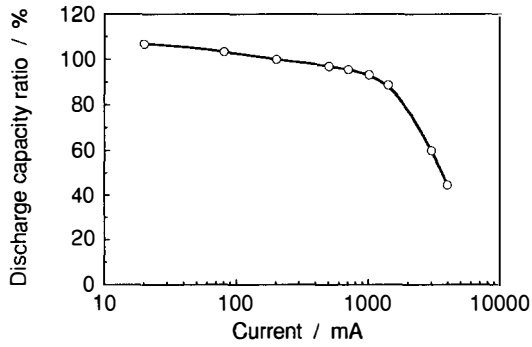

Fig. 13. A drain capability of a lithium ion rechargeable battery. Charge: max. limit 4.2 V, 1 A, 2.5 h. Discharge: 2.75 V cut off.

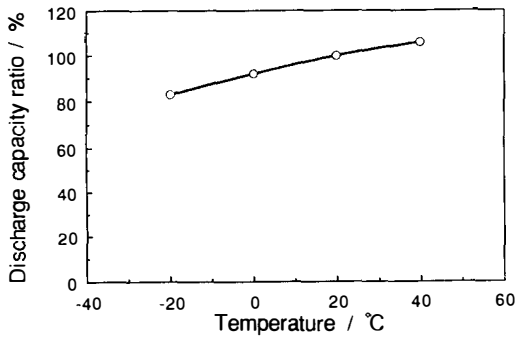

Fig. 14. A temperature dependence of discharge capacity. Charge: max. limit 4.2 V, 1 A, 2.5 h at 20°C; discharge: 2.75 cut off, 0.2 A (discharge capacity at 20°C = 100%).

4.2. Safety test

Since the lithium ion rechargeable battery includes no metallic lithium, it is expected to be a fairly safe and reliable battery. Safety tests such as crushing, nail penetration, overcharging and external short-circuiting were performed after charge–discharge cycling [19]. The battery was completely safe against crushing. The maximum temperature monitored at the outer can of the cell was only in the temperature range of 78 to 98°C though the cell was fully charged.

For the nail penetration test, a sharp metal spike of 4 mm in diameter and 35 mm in length was used. The cell temperature increased to the range of 77 to 105°C and only leakage of the electrolyte or only evolution of gas was initially observed. The more cycled cells tend to be safer: no gas evolution was observed after several tens of cycles.

Fig. 16 shows the changes in voltage and tempera-

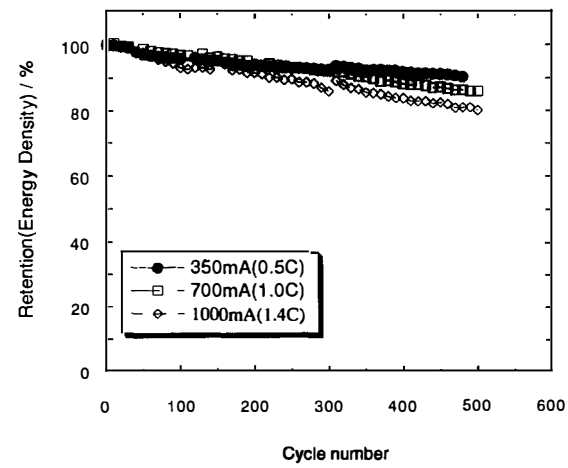

Fig. 15. Cycle performances of a lithium ion rechargeable battery.

RJ Technology Exhibit 2014
Apple Inc. v. RJ Technology LLC
IPR2023-01350, Page 7 of 10

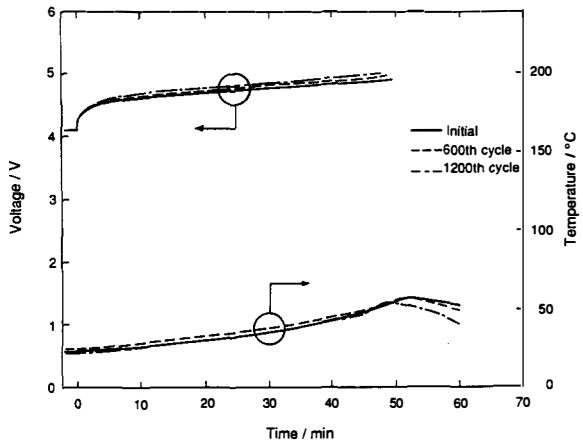

Fig. 16. Changes of voltage and temperature for several cycled cells in case of overcharging with no voltage limiting.

ture at battery overcharged with no charge limiting after several cycles. The anti-overcharging safety device was activated about 50 min after starting the overcharging, and the batteries died safely.

Changes of current and temperature batteries short-circuited after several cycles are shown in Fig. 17. The rush current smoothly decreases and the batteries are kept safe. In both cases of overcharging and short-circuiting, the maximum temperature of more cycled batteries is lower than that of less cycled batteries. This phenomenon proves that lithium ion rechargeable batteries become safer in accordance with charge–discharge cycling.

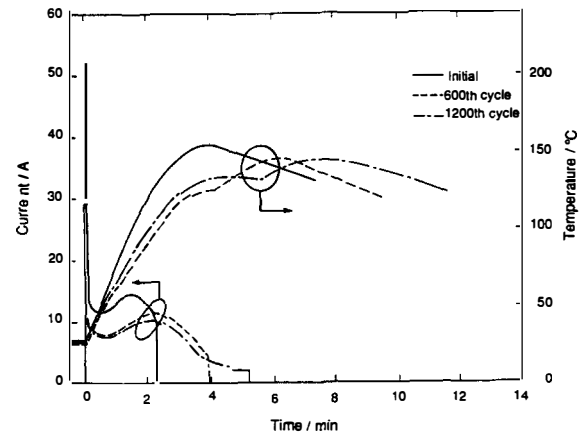

Fig. 17. Changes of current and temperature for several cycled cells in case of short circuit.

Table 1
Results of safety tests.

Test	Result
Penetration	No fire, no explosion
Crush	No fire, no explosion
Drop(1 m, 10 m)	No fire, no explosion
Overcharge(±35 V:46 A)	No fire, no explosion
Overcharge(1 A, 3 A)	No fire, no explosion
Short circuit	No fire, no explosion
Incineration	No explosion
Overheating	No explosion
Dipping in salt water	No fire, no explosion
Dipping in boiling water	No fire, no explosion
Dipping in an oil bath (180°C)	No fire, no explosion
Dipping in a solder bath	No fire, no explosion
High pressure test	No fire, no explosion
High altitude simulations	No fire, no explosion
Drilling	No fire, no explosion
Heating in a microwave oven	No fire, no explosion

Results of safety test are summarized in Table 1.

5. Characterization of the cycle life

It is very important to investigate the degradation mechanism of the lithium ion rechargeable battery during charge–discharge cycling to improve properties. Impedance analyses were performed in order to determine which composition caused the capacity degradation during cycling. Fig. 18 shows Cole–Cole plots of the cell charged up to 4.2 V. The impedance spectra consist of two semi-circles. The larger one becomes larger with decreasing the cell voltage. Furthermore, the shape of Cole–Cole plots, obtained by using a cell with only a fully charged carbon electrode, is similar to the larger semicircle observed at the low frequency region shown in Fig. 18. Hence, it is concluded that the larger semicircle in the low frequency region is attributed to the charge transfer reaction at the carbon anode. On the other hand, since the smaller semicircle becomes larger with decreasing the electrode surface area of the $LiCoO_2$ cathode, it is considered that the smaller one is attributed to the cathode. As for the smaller one, since the semicircle did not become larger with decrease in the cell voltage, the semicircle may not have been caused by the charge transfer resistance, but the impedance of

RJ Technology Exhibit 2014
Apple Inc. v. RJ Technology LLC
IPR2023-01350, Page 8 of 10

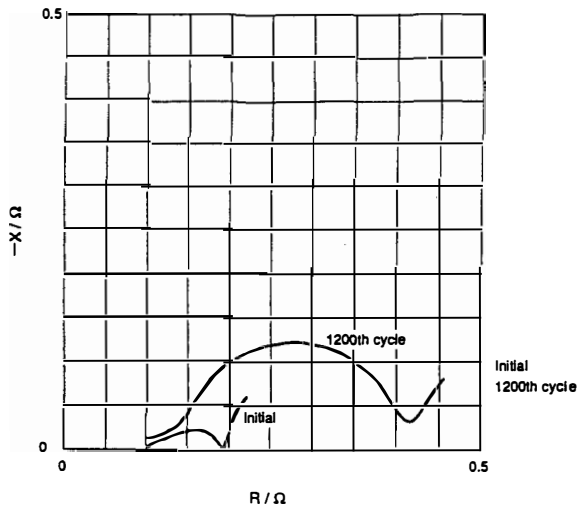

	Impedance	
	Cathode	Anode
Initial	32.3mΩ	61.5
1200th Cycle	38.5	269

Fig. 18. Impedance spectra of electrodes at initial and after 1200 cycles.

surface layer, so called solid electrolyte interphase (SEI), formed on the cathode surface.

As shown in Fig. 18, with increasing charge–discharge cycle number, the semi-circle assigned to the anode gradually became larger. Therefore, it is considered that the increase in charge transfer resistance at the anode would cause the decrease of the discharge capacity. Moreover, it is also found that by using PC+DEC/$LiPF_6$ the deterioration of $LiCoO_2$ cathode does not occur since the semicircle, assigned to the cathode, is almost constant with increasing charge–discharge cycle number.

By using SEM, EDX, AES and XPS analyses, it was found that a thin film of compounds, which consists mainly of lithium, carbon, oxygen and fluorine, was formed on the carbon surface during charge and discharge cycles. This film already exists on the carbon electrode after the initial charge and discharge cycle, and grows on the carbon surfaces with increasing number of cycles. Furthermore, using the solid state NMR, it was also found that lithium in the carbon anode material of fully charged cell remains in the ionic state, even after charge and discharge cycling [20].

These characterizations explain that the degradation of the performance of lithium ion rechargeable batteries during cycling is mainly caused by the deterioration of the carbon. The film (SEI) decreases the active surface area and hampers the rapid diffusion of the lithium ions [21].

6. Conclusion

The lithium ion rechargeable battery is suitable for many portable electronic equipment because of the high energy density, light weight and the long cycle life. Since lithium exists in the nonmetalic state in this battery even after charge–discharge cycles, these batteries are very safe against abuse, such as crushing and nail penetration. With a current breaker device and a vent mechanism provided for an abnormal rise of internal pressure, Sony's batteries are safe even under overcharging and short circuit conditions. The degradation of the carbon material with charge–discharge cycling is caused by the formation of the non-active thin film on the surface of the carbon anode.

Table 2
Performances of lithium ion rechargeable batteries.

Type batteries	Vol. (cm^3)	Weight (g)	Operation voltage (V)	Capacity (mAh)	Energy capacity (Wh)	Energy density		Cycle life in 100% DOD (cycles)	Self discharge (after 1 month) (%/(°C))	T (°C)	
						per vol [a]	per wt [b]			charge	discharge
14500	7.5	18	3.6	450	1.62	216	90	1200	8(23)	0~45	−20~60
20500	16.5	39	3.6	1200	4.32	261	110	1200	8(23)	0~45	−20~60
18650	17.06	40	3.6	1200	4.32	253	108	1200	8(23)	0~45	−20~60

[a] Wh/l; [b] Wh/kg.

RJ Technology Exhibit 2014
Apple Inc. v. RJ Technology LLC
IPR2023-01350, Page 9 of 10

The analysis of the film is very important in order to choose carbon and electrolyte materials suitable for the lithium ion rechargeable battery.

We have already achieved the energy density of 260 Wh/l and 110 Wh/kg in 20500 size cell. Table 2 summarizes the characteristics of the lithium ion rechargeable batteries which are available on the market.

Acknowledgements

The author thanks K. Tunoda for supporting this work. He is also indebted to Dr. K. Sekai and H. Imoto for useful discussions about the electrode materials and SEI.

References

[1] T. Nagaura, M. Nagamine, I. Tanabe and N. Miyamoto, Prog. Batt. Solar Cells 8 (1989) 84.
[2] T. Nagaura and K. Tozawa, Prog. Batt. Solar Cells 9 (1990) 209.
[3] K. Mizushima, P.C. Jones, P.J. Wiseman and J.B. Goodenough, Mat. Res. Bull. 15 (1980) 783.
[4] K. Mizushima, P.C. Jones, P.J. Wiseman and J.B. Goodenough, Solid State Ionics 3/4 (1981) 171.
[5] A. Mendiboure, C. Delmas and P. Hagenmuller, Mater. Res. Bull. 19 (1984) 1383.
[6] J.B. Goodenough and K. Mizushima, US Patent No. 4302518/2087858 (1981).
[7] T. Ozuku, M. Kitagawa and T. Hirai, J. Electrochem. Soc. 137 (1990) 769.
[8] T. Nagaura, JEC Battery Newsletter 2 (1991) 17.
[9] K. Sekai, H. Azuma, A. Omaru, S. Fujita, H. Imoto, T. Endo, K. Yamaura and Y. Nishi, J. Power Sources 43–44 (1993) 241.
[10] R.E. Franklin, Proc. Roy. Soc. A 209 (1951) 196.
[11] M. Mohri, N. Yanagisawa, Y. Tajima, H. Tanaka, T. Mitaie, S. Nakajima, Y. Yoshimoto, T. Suzuki and H. Wada, J. Power Sources 26 (1989) 545.
[12] H. Imoto, H. Azuma, A. Omuru and Y. Nishi, in: 58th Meeting Electrochem. Soc. Japan, Noda, April 5–7 (1991) Ext. Abstr., 158.
[13] H. Azuma, A. Omaru and Y. Nishi, in: Fall Meeting Electrochem. Soc. Japan, Nagoya, Oct. 12–13 (1991) Ext. Abstr. 132.
[14] A. Omaru, H. Azuma, M. Aoki and Y. Nishi, in: Fall Meeting Electrochem. Soc. Japan, Nagoya, Oct. 12–13 (1991) Ext. Abstr. 132.
[15] H. Imoto, A. Omaru, H. Azuma and Y. Nishi, Proc. Symp. on Lithium Batteries, PV 93-24 (1992) 9.
[16] A. Omaru, H. Azuma, M. Aoki, A. Kita and Y. Nishi, Proc. Symp. on Lithium Batteries, PV 93-24 (1992) 21.
[17] S. Fujita, A. Yasuda and Y. Nishi, Proc. Symp. on Primary and Secondary Lithium Batteries PV 91-3 (1991) 262.
[18] S. Mashiko, M. Yokokawa and T. Nagaura, in: 32nd Battery Symp. Japan, Kyoto, Sept. 17–19 (1991) Ext. Abstr. p. 31.
[19] K. Ozawa and M. Yokokawa, The International Rechargeable Battery Seminar, Florida, March 2–4 (1992).
[20] K. Tanaka, M. Itabashi, M. Aoki, S. Hiraka, M. Kataoka, K. Sataori, S. Fujita, K. Sekai and K. Ozawa, 184th ECS Fall Meeting (1993).
[21] R. Fong, U. von Sacken and J.R. Dahn, J. Electrochem. Soc. 137 (1990) 2009.

RJ Technology Exhibit 2014
Apple Inc. v. RJ Technology LLC
IPR2023-01350, Page 10 of 10